Euro. Jnl of Applied Mathematics (2000), *vol.* 11, *pp.* 81–94. Printed in the United Kingdom

© 1999 Cambridge University Press

Stress-controlled shear waves in a saturated granular medium

BRIAN T. HAYES and DAVID G. SCHAEFFER†

Department of Mathematics and Center for Nonlinear and Complex Systems, Duke University, Durham, NC 27708-0320, USA

(*Received: 16 June 1998; revised 4 August 1999*)

We study plane shear waves in a continuum model for a saturated soil, assuming a hypoplastic flow rule. Following an earlier paper on velocity-controlled waves [1], we now specify a time-periodic stress disturbance on the boundary of a semi-infinite medium. As before, the stress saturates, tending at large times to a position-independent value, away from the boundary. By contrast, the dependence of this asymptotic state on the boundary data is strikingly different: in the previous case, this dependence was wildly discontinuous, while here it is very simple and smooth.

1 Introduction

In this paper, we study an initial/boundary value problem in the quarter-plane $\{x, t \geqslant 0\}$ for the system

$$\begin{aligned} \partial_t v &= \partial_x \sigma, \\ \partial_t \sigma &= a\,\partial_x v + b|\partial_x v|, \end{aligned} \tag{1.1}$$

where the constants a and b satisfy $a > b > 0$. We assume constant initial conditions

$$v(x,0) = 0 \quad \text{and} \quad \sigma(x,0) = \sigma_0 < 0, \tag{1.2}$$

and boundary conditions

$$\sigma(0,t) = f(t), \tag{1.3}$$

where $f(t)$ is a τ-periodic square wave. For example, given $\mu \in (0,1)$, consider

$$f(t) = \begin{cases} \sigma_-, & n\tau < t < (n+\mu)\tau, \\ \sigma_+, & (n+\mu)\tau < t < (n+1)\tau, \end{cases} \tag{1.4}$$

for $n = 0, 1, 2, \ldots$, where $\sigma_- < \sigma_+ < 0$. (In §4 we shall also consider boundary data with $\sigma_\pm$ interchanged.)

As shown by Osinov & Gudehus [2], system (1.1) arises in the description of small-amplitude plane shear waves[1] propagating in a three-dimensional soil, assuming a

† Research supported by NSF Grant DMS-9504577.

[1] Osinov [4, 5] derived (1.1) in studying longitudinal waves. Indeed, as the following discussion shows, (1.1) may be expected in a variety of problems. Equations (1.1) consist of a conservation law and a constitutive relation. In so-called *rate independent* constitutive relations for soils, stress rate depends upon strain rate as a homogeneous function of degree one. Such a functional relationship, if not linear, is singular at the origin in strain-rate space. The absolute value function in (1.1) reflects this singularity.

https://doi.org/10.1017/S0956792599004064 Published online by Cambridge University Press

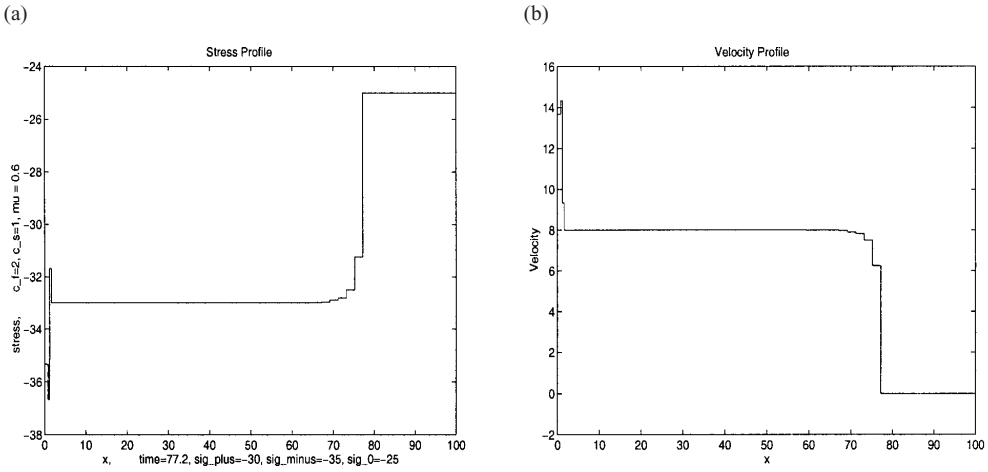


FIGURE 1. (a) Stress profile for the stress-controlled case; (b) velocity profile.

hypoplastic flow rule (see also Gudehus [3]). The dependent variables v and σ in (1.1) represent a component of velocity and a component of stress,[2] respectively.

We studied an analogous problem with an oscillating *velocity*, rather than stress, prescribed at the boundary [1]. Since the analysis is similar in both cases, we refer back to our earlier work in several places, for details of the construction. As the first such reference, we recall that, depending on the sign of $\partial_x v$, system (1.1) admits discontinuous solutions with speeds $\pm c_f$ and $\pm c_s$, where

$$c_f = \sqrt{a+b} \quad \text{and} \quad c_s = \sqrt{a-b}. \tag{1.5}$$

Waves with speeds $+c_f$ or $+c_s$ will be called fast or slow positive waves, respectively; waves with speeds $-c_f$ or $-c_s$, fast or slow negative waves.

As in the velocity-controlled case, the solution of (1.1)–(1.4) exhibits qualitatively different behaviour at large times, in four different regions. Proceeding from right to left, there are:

1. The *quiescent region*: the solution is $(v, \sigma) = (0, \sigma_0)$, because the effect of the boundary disturbance has yet to be felt.
2. The *propagation region*: a sequence of positive waves escapes off to spatial infinity, as $t \to \infty$.
3. The *asymptotic region*: behind the propagating waves, as $t \to \infty$, the velocity and stress tend to constants v_∞ and σ_∞, respectively, which are independent of x.
4. The *interaction region*: in a strip of constant width along the boundary, the solution exhibits complicated x-dependence and periodic t-dependence.

We illustrate these behaviours in Figures 1(*a*) and (*b*), which show stress and velocity profiles, respectively, at time $t = 77.2$. In these figures, the just mentioned regions intersect

[2] The assumption that σ_+, σ_0 and σ_- are all negative arises from the physical origins of the problem: without this constraint, the sign of b in (1.1) would be negative, or possibly even position-dependent.

https://doi.org/10.1017/S0956792599004064 Published online by Cambridge University Press

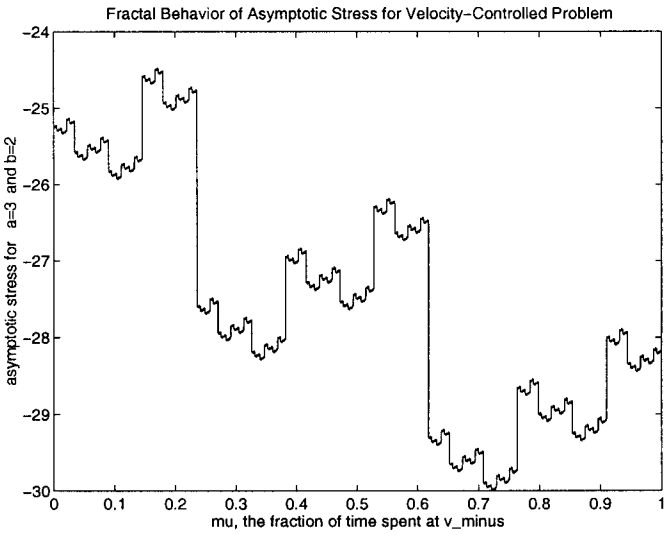


FIGURE 2. Discontinuous dependence of σ_∞ on μ in the *velocity-controlled* case, as in Hayes & Schaeffer [1].

the line $\{t = 77.2\}$ in the following x-intervals: the quiescent region is $x > 77.2$, the propagation region is $65 < x < 77.2$, the asymptotic region is $x_I = 4 < x < 65$ and the interaction region is $0 \leqslant x < 4$. We have identified the boundary between the asymptotic and propagation regions visually, using the figures; to define this boundary analytically, one must specify a degree of accuracy for the convergence in the asymptotic region. These profiles were computed numerically, with wave speeds $c_f = 2$ and $c_s = 1$, initial data $\sigma_0 = -25$, and boundary data $\sigma_+ = -30$, $\sigma_- = -35$, with $\mu = 0.6$.

Despite the similarities with the velocity-controlled case, the differences are far more dramatic. Most notably, in our earlier paper [1] the stress σ_∞ in the asymptotic region had a discontinuous, fractal dependence on the parameters[3] μ, a and b; see Figure 2 (and Figures 3 and 9 of Hayes & Schaeffer [1]). By contrast, in the present case, σ_∞ is independent of a and b; and as a function of μ, it is given simply by the convex combination

$$\sigma_\infty = \mu\,\sigma_- + (1-\mu)\sigma_+; \tag{1.6}$$

in particular, σ_∞ is independent of the initial stress σ_0. Note that in Figure 1(*a*), we have $\sigma_\infty = -33$, as predicted by (1.6).

The physical origin of this discrepancy, between smooth dependence on stress-controlled boundary data and violently discontinuous dependence on velocity-controlled data, remains an open question. To determine whether this phenomenon is an artifact of the model (1.1) or mimics the true, physical behaviour of saturated soils (and, if so, why?), will probably require actual experiments.

Two other, minor, differences between the two cases are:

[3] Strictly speaking, the parameter in Hayes & Schaeffer [1] describing the shape of the boundary data was $1-\mu$, which was called λ there.

https://doi.org/10.1017/S0956792599004064 Published online by Cambridge University Press

- In the present case, the convergence to the asymptotic state is faster than in Hayes & Schaeffer [1].
- With the possible exception of one or two initial *fast* positive waves, all escaping waves in the present problem are *slow* waves, rather than all fast waves, as in Hayes & Schaeffer [1].

For ease of exposition, in the first three sections of this paper we temporarily restrict ourselves to a special case by making the additional, technical, assumption that

$$\sigma_+ < \sigma_0; \tag{1.7}$$

this guarantees that *all* waves in the propagation region are slow waves.

The remainder of this paper is organized as follows. In §2 we discuss the construction of the solution of (1.1)–(1.4), focusing on what is different from the construction in Hayes & Schaeffer [1]. In §3 we derive the properties of the solution described above, in the special case. In §4, we deal with the general case – specifically, removing the restriction (1.7) and allowing $\sigma_\pm$ to occur in either order in (1.4); despite some differences, the conclusions above still hold.

2 Construction of the solution

As in Hayes & Schaeffer [1], the solution of (1.1)–(1.4) will be constructed by combining piecewise-constant solutions of (1.1) containing one jump, i.e. solutions of the form

$$v(x,t) = v_R, \quad \sigma(x,t) = \sigma_R, \quad \text{if } x > x_0 + st$$

and

$$v(x,t) = v_L, \quad \sigma(x,t) = \sigma_L, \quad \text{if } x < x_0 + st,$$

where $s = \pm c_f$ or $\pm c_s$. For a given state (v_R, σ_R) on the right, the states (v_L, σ_L) arising from such solutions lie on four semi-infinite rays in the v,σ-plane (see Figure 3). Each ray corresponds to one of the four types of waves:[4] specifically, we define the wave curves

$$\begin{aligned}
\mathscr{P}_f &= \{(v,\sigma): \sigma = \sigma_R + c_f(v_R - v), \quad v \leqslant v_R\},\\
\mathscr{P}_s &= \{(v,\sigma): \sigma = \sigma_R + c_s(v_R - v), \quad v \geqslant v_R\},\\
\mathscr{N}_f &= \{(v,\sigma): \sigma = \sigma_R - c_f(v_R - v), \quad v \leqslant v_R\},\\
\mathscr{N}_s &= \{(v,\sigma): \sigma = \sigma_R - c_s(v_R - v), \quad v \geqslant v_R\}.
\end{aligned}$$

In this paper, deviating from Hayes & Schaeffer [1], we shall measure the strength of a wave by the *stress* jump across it, $\Gamma = |\sigma_R - \sigma_L|$.

The solution of (1.1)–(1.4) is piecewise-constant in x and t, with jumps of the above type along a countable family of line segments

$$x = a_j + c_j t \tag{2.1}$$

for $j = 1, 2, 3, \ldots$; here $c_j = \pm c_f$ or $\pm c_s$, and t is restricted to an appropriate interval $\boldsymbol{I}_j \subset \boldsymbol{R}^+$.

[4] Our notation for waves is changed from Hayes & Schaeffer [1]: the waves that we denote by $\mathscr{P}_f$, $\mathscr{P}_s$, $\mathscr{N}_f$ and $\mathscr{N}_s$ here were written $\mathscr{F}_+$, $\mathscr{S}_+$, $\mathscr{F}_-$ and $\mathscr{S}_-$, respectively, in Hayes & Schaeffer [1]. This change in notation shifts the emphasis onto the more important dichotomy between right- and left-moving waves, away from the dichotomy between fast and slow waves.

https://doi.org/10.1017/S0956792599004064 Published online by Cambridge University Press

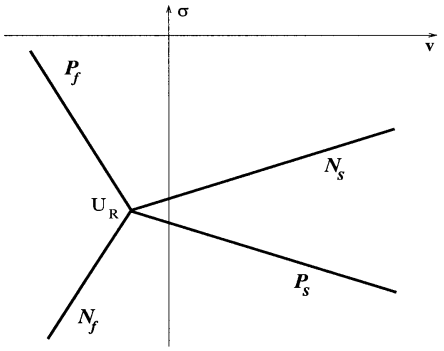


FIGURE 3. Wave curves in the v, σ-plane.

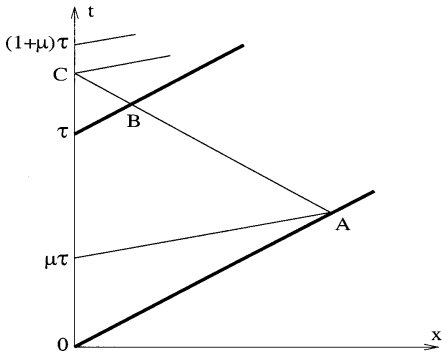


FIGURE 4. Network of waves in the x, t-plane for small times.

the network of waves (2.1) is sketched, for small times, in Figure 4. In the figure, $\mathscr{P}_s$ waves are shown in bolder type, both for ease of recognition and because, as we shall see in §3, these waves form the 'backbone' of the solution.

Endpoints of the line segments (2.1) are associated with one of the following phenomena:

1. Emission of a new positive wave, either fast or slow, at the boundary (e.g. this occurs at times $0, \mu\tau, \tau, \ldots$ in Figure 4).
2. Reflection of a negative wave at the boundary as a positive wave (e.g. this occurs at point C in Figure 4).
3. Collision of two waves (e.g. this occurs at points A and B in Figure 4).

For discussion of case (3), it is useful to define the parameter[5]

$$\beta = \frac{c_f - c_s}{2c_f}; \tag{2.2}$$

note that $0 < \beta < 1/2$. To continue the solution beyond a collision, one must solve a Riemann problem. (For these Riemann problems to have unique solutions, we must rule

[5] The analogous parameter in Hayes & Schaeffer [1] was $\alpha = (c_f - c_s)/(c_f + c_s)$. The fact that $\beta < \alpha$ hastens the convergence of the solution in the present case.

https://doi.org/10.1017/S0956792599004064 Published online by Cambridge University Press

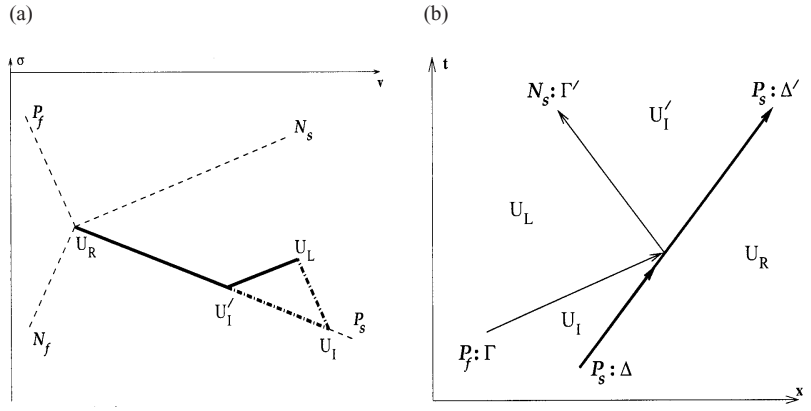


FIGURE 5. (a) A $\mathscr{P}_f$–$\mathscr{P}_s$ collision in the v, σ-plane; (b) a $\mathscr{P}_f$–$\mathscr{P}_s$ collision in the x, t-plane.

out would-be solutions that have both fast and slow waves of the same family; see the appendix of Hayes & Schaeffer [1] for further discussion of this point, including a viscosity argument that such multiple-wave solutions are unphysical.) Figure 5 illustrate this continuation for a key example – the collision of fast and slow positive waves, such as occurs at point A in Figure 4. The right state U_R, left state U_L, and precollision intermediate state U_I are given; the problem is to find the postcollision intermediate state U_I'. Let the incoming $\mathscr{P}_f$ wave have strength Γ and the incoming $\mathscr{P}_s$ wave have strength Δ, and suppose that

$$(1-\beta)\Gamma < \Delta. \tag{2.3}$$

Then, by a calculation similar to the proof of Lemma 3.3 of Hayes & Schaeffer [1], we find that the outgoing waves are *both* slow waves, one negative and one positive, whose strengths are

$$\Gamma' = \beta\Gamma, \quad \Delta' = \Delta - (1-\beta)\Gamma, \tag{2.4}$$

respectively. The outgoing waves are therefore weaker than the incoming waves.

The collisions of other combinations of waves that occur in solving (1.1)–(1.4) are simpler. For example, at a collision of slow positive and slow negative waves, such as that which occurs at point B in Figure 4, both waves continue without change in type or strength. Using notation analogous to that of Figure 5(a), the four states U_R, U_I, U_L and U_I' lie on the vertices of a parallelogram in the v, σ-plane.

In case (2), to continue the solution, one must solve a quarter-plane problem. The reflection of an incident $\mathscr{N}_s$ wave as a $\mathscr{P}_f$ wave is illustrated in Figure 6. In the figure, σ_B refers to the value of σ specified by the boundary condition (1.3), either σ_+ or σ_-, depending on the time at which the reflection occurs. Since we measure wave strengths by the *stress* jump, the reflected wave has the same strength as the incident wave.

Case (1), the emission of a new positive wave, is similar to case (2). At times $t = (n+\mu)\tau$, for $n = 0, 1, 2, \ldots$, the boundary value jumps *up*, so that $\sigma_R < \sigma_L$, and hence a $\mathscr{P}_f$ wave is emitted; at times $t = n\tau$, the boundary value of σ jumps *down*, so a $\mathscr{P}_s$ wave is emitted. Each of these waves is emitted with strength $\sigma_+ - \sigma_-$, except the wave starting at time zero; the latter wave is emitted with strength $\sigma_0 - \sigma_-$, and by (1.7), this is a $\mathscr{P}_s$ wave of greater strength.

https://doi.org/10.1017/S0956792599004064 Published online by Cambridge University Press

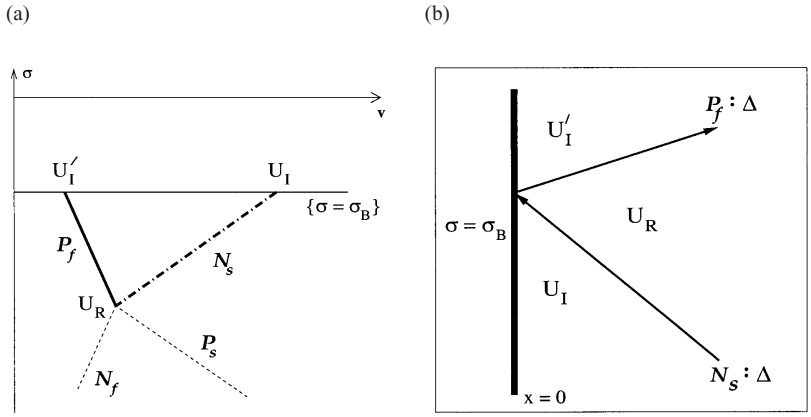


FIGURE 6. (a) Reflection of $\mathscr{N}_s$ wave in the v, σ-plane; (b) reflection in the x, t-plane.

3 Properties of the solution

Our main results, for the special case, are stated in the following theorem. In this theorem, square brackets denote the greatest-integer function.

Theorem 3.1. *Under the additional hypothesis* (1.7) *the solution of* (1.1)–(1.4) *has the following properties:*

(a) *All wave interactions are confined to the strip* $\{0 \leqslant x < x_I\}$, *where*

$$x_I = \frac{c_f c_s}{c_f - c_s}\tau. \tag{3.1}$$

(b) *For* $x > c_s t$, *the solution remains in its quiescent initial state*, $(v, \sigma) = (0, \sigma_0)$.

(c) *For any fixed* $x > x_I$, *as* $t \to \infty$, *the stress and velocity tend to constant states*,

$$\text{(a)}\ \ \sigma_\infty = \mu\sigma_- + (1-\mu)\sigma_+, \quad \text{(b)}\ \ v_\infty = -(\sigma_\infty - \sigma_0)/c_s. \tag{3.2}$$

(d) *Between the quiescent region in* (b) *and the asymptotic region in* (c) *are a sequence of non-interacting* $\mathscr{P}_s$ *waves, whose strengths decrease from right to left. For the* $\mathscr{P}_s$ *wave emitted from the boundary at time* $t = n\tau$, $n = 1, 2, \ldots$, *we have the bound*

$$|\sigma_R - \sigma_L| \leqslant (\sigma_+ - \sigma_-)\beta^{n/N_{max}}, \tag{3.3}$$

where β *is given by* (2.2) *and* $N_{max} = [1/\beta]$.

Despite significant differences, the proof of Theorem 3.1 is very similar to the corresponding proof in Hayes & Schaeffer [1]. For the purposes of exposition, we divide the proof of Hayes & Schaeffer [1] into three steps:

Step 1: define and analyse three kinds of wave interactions.
Step 2: make an inventory of all waves in the solution.
Step 3: estimate the strength of escaping waves.

We sketch the proof of Theorem 3.1 by (i) describing the changes in each of these three steps that are needed in the present context, and (ii) performing a fourth step, which

https://doi.org/10.1017/S0956792599004064 Published online by Cambridge University Press

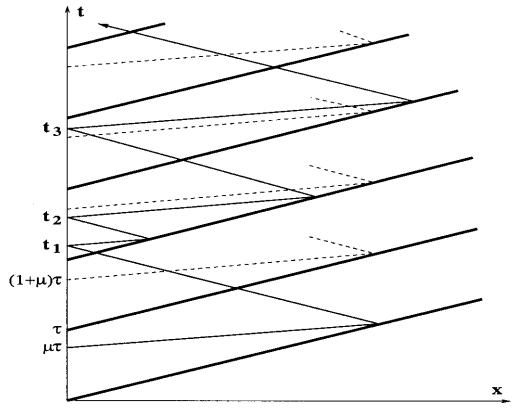


FIGURE 7. Path, $X(t)$, of the initial $\mathscr{P}_f$–$\mathscr{N}_s$ wave in the x, t-plane.

simplifies formula (3.10) in a way that is not possible in the context of Hayes & Schaeffer [1].

Step 1: we define the following three types of wave interactions:

Type I: a $\mathscr{P}_f$ wave of strength Γ overtakes a $\mathscr{P}_s$ wave of strength Δ, where (2.3) holds, i.e. $(1-\beta)\Gamma < \Delta$.
Type II: a $\mathscr{N}_s$ wave and a $\mathscr{P}_f$ wave collide.
Type III: a $\mathscr{N}_s$ wave and a $\mathscr{P}_s$ wave collide.

These three types of wave interactions are the same as in Hayes & Schaeffer [1], except that here, at an interaction of Type I, inequality (2.3) bounds the strength of the $\mathscr{P}_s$ wave from *below* rather than above. (Furthermore, the strength of a wave is now measured by the jump in stress across a wave.) In solving (1.1)–(1.4), provided (1.7) holds, only interactions of one of these three types occur. In particular, no $\mathscr{N}_f$ waves are generated, and inequality (2.3) is always satisfied at a $\mathscr{P}_f$–$\mathscr{P}_s$ collision. As in Hayes & Schaeffer [1], the proof of this statement is most conveniently deferred until Step 3, below.

In Lemma 3.3 of Hayes & Schaeffer [1], the positive and negative waves emerging from the three types of wave interactions were catalogued. For the present paper, this task was already performed, by example, in §2. The main difference now comes from inequality (2.3): at an interaction of Type I, the positive wave that emerges from the collision is a *slow* wave (see Figure 5). At interactions of Types II and III, both waves continue without change in type or strength.

It follows from the above discussion that (i) the $\mathscr{P}_s$ waves emitted at time $t = n\tau$, for $n = 0, 1, 2, \ldots$, continue beyond any collisions they may suffer, and (ii) no new $\mathscr{P}_s$ waves are generated by collisions – only existing $\mathscr{P}_s$ waves are propagated past the collisions. Indeed,

$$x = c_s(t-n\tau), \quad n = 0, 1, 2, \ldots, \tag{3.4}$$

is a complete listing of the slow positive waves that occur in the solution of (1.1)–(1.4).

Step 2: consider the first $\mathscr{P}_f$ wave, which is emitted from the boundary at time $t = \mu\tau$ (see Figure 7). When this wave overtakes the $\mathscr{P}_s$ wave emitted at time zero, we regard the $\mathscr{N}_s$

https://doi.org/10.1017/S0956792599004064 Published online by Cambridge University Press

wave that emerges from the collision as a continuation of the incident $\mathscr{P}_f$ wave. Similarly, when this $\mathscr{N}_s$ wave reflects from the boundary, we regard the $\mathscr{P}_f$ wave that emerges as a continuation of the incident wave. The trajectory of the first $\mathscr{P}_f$ wave, continued in this way, is an infinite broken line,

$$x = X(t), \quad t \geqslant \mu\tau, \tag{3.5}$$

the speeds of the various segments alternating between $+c_f$ and $-c_s$.

The time t_1 when $X(t)$ first reflects from the boundary (see Figure 7) is easily calculated as

$$t_1 = \frac{2c_f}{c_f - c_s}\mu\tau = \beta^{-1}\mu\tau,$$

where we have recalled (2.2). To locate t_1 within a period of the boundary data, we write $t_1 = (\mu_1 + N_1)\tau$, where $N_1 = [\beta^{-1}\mu]$ and $\mu_1 = \beta^{-1}\mu - N_1$. Continuing inductively, we conclude that $X(t)$ reflects from the boundary for the jth time when

$$t = (\mu_j + N_j + \ldots + N_1)\tau,$$

where

$$\text{(a)}\ \ N_j = [\beta^{-1}\mu_{j-1}] \quad \text{(b)}\ \ \mu_j = \beta^{-1}\mu_{j-1} - N_j. \tag{3.6}$$

Note that $0 \leqslant \mu_j < 1$.

We claim that $X(t) \leqslant x_I$, where x_I is given by (3.1). As may be seen from Figure 7, the first collision of $X(t)$ occurs at $x = \{c_f c_s/(c_f - c_s)\}\mu\tau$; thus, for $0 \leqslant t \leqslant t_1$,

$$X(t) \leqslant \frac{c_f c_s}{c_f - c_s}\mu\tau < x_I,$$

the last inequality because $\mu < 1$. Similarly, $X(t) < x_I$ for $t_{j-1} \leqslant t \leqslant t_j$ because $\mu_{j-1} < 1$, and the claim follows.

Given the assumption (1.7), a fast wave emitted at a later time, say $t = (n + \mu)\tau$, undergoes the same sequence of interactions as the first such wave, and follows the same trajectory $X(\cdot)$, only delayed by time $n\tau$, i.e.

$$x = X(t - n\tau), \quad t \geqslant (n + \mu)\tau. \tag{3.7}$$

Every wave interaction occurs along one of the trajectories (3.7), which verifies part (a) of the theorem. Also, no fast waves escape the interaction region. Since the escaping waves are slow waves, the solution of (1.1)–(1.4) is quiescent for $x < c_s t$. Finally, if σ tends to an asymptotic value σ_∞ as $t \to \infty$, then v tends to the value given by (3.2*b*), since the $\mathscr{P}_s$ wave curve through $(0, \sigma_0)$ is the straight line with equation

$$v = -(\sigma - \sigma_0)/c_s, \quad v \geqslant 0.$$

Step 3: let us tabulate the interactions of Type I suffered by the slow positive waves in crossing the interaction region (see Figure 7):

- The first N_1 such waves,[6] emitted at times $0, \tau, \ldots, (N_1 - 1)\tau$, suffer exactly one interaction of Type I, this with a $\mathscr{P}_f$ wave that has not yet been reflected from the boundary.

[6] It is possible for N_1 and/or subsequent N's to equal zero (e.g. see Figure 7, where $N_2 = 0$), but the claims made here are still valid.

https://doi.org/10.1017/S0956792599004064 Published online by Cambridge University Press

- The next N_2 such waves, emitted at times $N_1\tau, (N_1+1)\tau, \ldots, (N_1+N_2-1)\tau$, suffer exactly two interactions of Type I, one with a $\mathscr{P}_f$ wave that has not yet been reflected, and one with a wave that has undergone one reflection.

Proceeding to the general case:

- The waves emitted at times $(N_1+\ldots+N_{j-1})\tau, \ldots, (N_1+\ldots+N_j-1)\tau$ suffer exactly j interactions of Type I, with $\mathscr{P}_f$ waves that have undergone $0, \ldots, j-2$, and $j-1$ reflections.

We estimate the effect of these interactions on wave strengths by applying (2.4) repeatedly (i) after j reflections from the boundary, a fast positive wave (with initial strength $\sigma_+-\sigma_-$) has strength $(\sigma_+-\sigma_-)\beta^j$; and (ii) a slow positive wave with initial strength Δ, that undergoes j interactions of Type I prior to escaping, emerges with strength

$$\begin{aligned}\Delta' &= \Delta-(1-\beta)(\sigma_+-\sigma_-)(1+\beta+\ldots+\beta^{j-1})\\ &= \Delta-(\sigma_+-\sigma_-)(1-\beta^j).\end{aligned} \tag{3.8}$$

All slow positive waves, except the one emitted at time zero, have initial strength $\sigma_+-\sigma_-$; substituting into (3.8), we obtain

$$\Delta' = (\sigma_+-\sigma_-)\beta^j. \tag{3.9}$$

The wave emitted at time zero has initial strength $\sigma_0-\sigma_-$, which by (1.7) is greater than that of later waves; if it suffers j interactions, on escaping it has strength

$$\sigma_0-\sigma_++(\sigma_+-\sigma_-)\beta^j.$$

Summing the jumps across all escaping, slow positive waves, we calculate, by grouping waves that suffer the same number of interactions, that

$$\sigma_0-\sigma_\infty = \sigma_0-\sigma_++(\sigma_+-\sigma_-)\sum_{j=1}^{\infty} N_j\beta^j. \tag{3.10}$$

We argue two additional points, as previously [1]: (i) the analysis leading to (3.8) can be modified to show that (2.3) holds at any $\mathscr{P}_f$–$\mathscr{P}_s$ wave collision; and (ii) (3.3) can be derived from (3.9).

Step 4: up to this point, the present proof parallels that of earlier [1]; in particular, (3.10) is analogous to equation (3.9). In contrast to the previous case,[7] however, the summation in (3.10) has the simple closed form (3.11). Equation (3.2*a*) results from substitution of (3.11) into (3.10).

Lemma 3.2

$$\sum_{j=1}^{\infty} N_j\beta^j = \mu. \tag{3.11}$$

[7] The mathematical origin of this difference is that in (3.6), unlike the corresponding equation (3.2) [1], the mapping $\mu_{j-1}\mapsto\mu_j$ does not involve a reflection of the interval $[0,1]$. Physically, it is unclear why velocity- and stress-controlled boundary conditions should behave so differently. It would be interesting to see whether experimental studies on saturated soils show related behaviours.

https://doi.org/10.1017/S0956792599004064 Published online by Cambridge University Press

Proof We start by rewriting (3.6*b*);

$$\mu_{j-1} = N_j \beta + \beta \mu_j. \tag{3.12}$$

Although, strictly speaking, (3.12) is not meaningful for $j = 1$, in this case we have the defining relation for μ_1, N_1:

$$\mu = N_1 \beta + \beta \mu_1. \tag{3.13}$$

Starting with (3.13) and applying (3.12) inductively, we deduce that for any ℓ

$$\mu = \sum_{j=1}^{\ell} N_j \beta^j + \beta^\ell \mu_\ell,$$

and the lemma follows on letting $\ell \to \infty$.

This completes the proof of Theorem 3.1. □

4 More general boundary conditions

With general boundary data, the framework provided by Theorem 3.1 continues to apply, but some of the specifics change. Part (a) of the theorem remains valid without change. Regarding (b), in general the solution is quiescent only for $x > c_f t$. Regarding (c), in the asymptotic region, as $t \to \infty$, the stress still converges to the value given in (3.2*a*), but formula (3.2*b*) for the velocity suffers some modification. Regarding (d), there is still an infinite sequence of $\mathscr{P}_s$ waves, whose strengths decrease geometrically, escaping the interaction region; however, depending on data in the problem, either zero, one or two *fast* positive waves may escape before the infinite sequence of escaping slow waves takes over. In this section, we elaborate on these escaping fast waves.

We refer to the boundary data given by (1.4) as Case A, and to the boundary data with $\sigma_\pm$ interchanged,[8]

$$f(t) = \begin{cases} \sigma_+, & n\tau < t < (n+1-\mu)\tau, \\ \sigma_-, & (n+1-\mu)\tau < t < (n+1)\tau, \end{cases}$$

for $n = 0, 1, 2, \ldots$, as Case B; we drop assumption (1.7) in either case. We divide Case B into two subcases as follows:

Case B1: $\sigma_0 < \sigma_+$
Case B2: $\sigma_+ < \sigma_0$.

For a similar subdivision of Case A, we need the integer

$$k = \min\{j : \beta^{-j}\mu > 1\}. \tag{4.1}$$

[8] A similar permutation of v_+ and v_- in the *velocity-controlled* case of earlier [1] would scarcely affect the solution; in particular, both v_∞ and σ_∞ would be unchanged. By contrast, both v_∞ and σ_∞ depend upon the initial stress σ_0.

To see this invariance, recall that in the earlier paper [1], the initial escaping $\mathscr{P}_f$ wave had strength $|v_-|$. If, instead, we had started with $v(0, t) = v_+$, the just-mentioned initial jump, $|v_-|$, would be made up through a sequence, $n = 1, 2, \ldots$, of $\mathscr{P}_f$–$\mathscr{P}_s$ collisions involving the initial $\mathscr{P}_s/\mathscr{N}_s$ wave, each transmitting an *additional* strength of $\alpha^{n-1}(1-\alpha)|v_-|$. Since all escaping waves remain $\mathscr{P}_f$, the value of σ_∞ is also unaffected.

https://doi.org/10.1017/S0956792599004064 Published online by Cambridge University Press

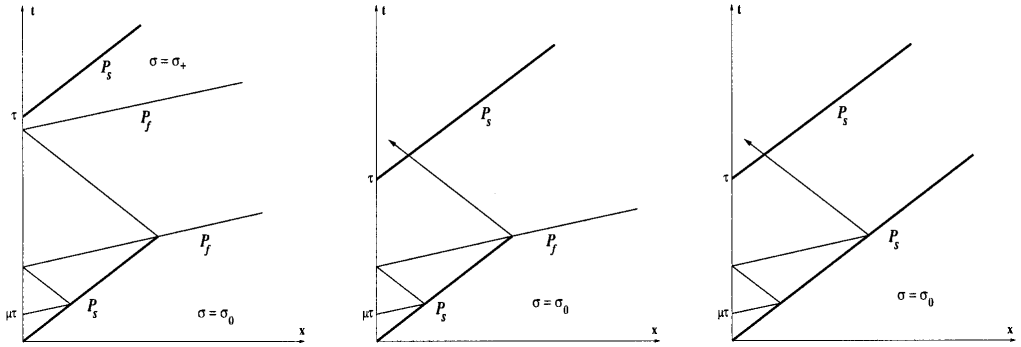


FIGURE 8. Case A1, two $\mathscr{P}_f$ waves (left); A2, one $\mathscr{P}_f$ wave (centre); and A3, no $\mathscr{P}_f$ waves (right). In Case A1, the integer k of (4.1) equals 3; in Cases A2 and A3, it equals 2.

To describe k in words and pictures, consider the broken-line trajectory (3.5) of the $\mathscr{P}_f$ wave emitted at time $\mu\tau$, as it bounces back and forth between a $\mathscr{P}_s$ wave starting from $x = 0$ at time zero and the boundary $\{x = 0\}$ (see Figure 8): if $X(t)$ reflects off the boundary at times $t_1, t_2, \ldots$, then k equals the subscript j of the first time such that $t_j > \tau$. Alternatively, we have $k = \min\{j: N_j > 0\}$, where for $j = 1, 2, \ldots$, the integer N_j is given by (3.6). Define

$$\Sigma_- = \sigma_+ - \beta^{k-1}(\sigma_+ - \sigma_-) \quad \text{and} \quad \Sigma_+ = \sigma_+ - \beta^k(\sigma_+ - \sigma_-).$$

Note that $\sigma_- \leqslant \Sigma_- < \Sigma_+ < \sigma_+$, with the equality $\sigma_- = \Sigma_-$ holding if and only if $k = 1$. To conclude, we divide Case A into three subcases as follows:

Case A1: $\sigma_0 < \Sigma_-$
Case A2: $\Sigma_- < \sigma_0 < \Sigma_+$
Case A3: $\Sigma_+ < \sigma_0$.

Case A3 includes the special case (1.4), (1.7), which was analysed in §3. Note that in Figure 8(*a*), for Case A1, we have shown the solution for the subcase $\sigma_- < \sigma_0$; if $\sigma_0 < \sigma_-$, the initial and second waves would both be *emitted* as $\mathscr{P}_f$ waves.

As noted above, much of Theorem 3.1 carries over to the general case. In the following result, we focus on the main difference between the special and general cases, i.e. escaping fast waves.

Proposition 4.1 *In Cases* A1, A2 *and* A3, *there are two, one and zero* $\mathscr{P}_f$ *waves that escape the interaction region, respectively; in Cases* B1 *and* B2, *there are one and zero such waves, respectively.*

To derive formula (3.2) for the asymptotic state, one must know the exact number of escaping fast waves, and their strengths, since the asymptotic state is obtained from the initial state $(0, \sigma_0)$ by summing the strengths of all escaping waves. However, complete analysis of all cases in this proposition is somewhat lengthy, so we merely indicate the highlights of the proof. Incidentally, given that there are so many possible combinations of escaping waves, we find it all the more surprising that the asymptotic stress σ_∞ is independent of the initial stress σ_0.

https://doi.org/10.1017/S0956792599004064 Published online by Cambridge University Press

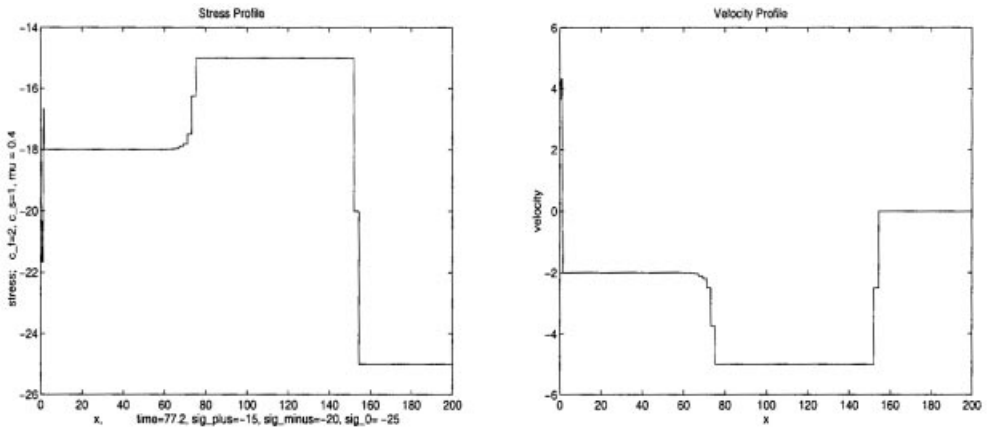


FIGURE 9. (a) Stress profile with two $\mathscr{P}_f$ waves, (b) velocity profile.

The analysis of Case B2 is completely analogous to that of §3. In Case B1, the wave emitted from the boundary at time zero is a *fast* positive wave; since no wave emitted later can overtake it, this wave escapes. However, there are no further complications in the analysis; in particular, (2.3) holds at all $\mathscr{P}_f$–$\mathscr{P}_s$ wave collisions.

Case A3 when $\sigma_+ < \sigma_0$ was analysed in §3. Case A1 when $\sigma_0 < \sigma_-$ is similar to Case B1 above: the first two waves, emitted at times zero and $\mu\tau$, are both fast waves, and these escape without undergoing any interactions. Therefore, in discussing Cases A1, A2 and A3, *we make the additional assumption* that

$$\sigma_- < \sigma_0 < \sigma_+;$$

in particular, the wave emitted at time zero is a *slow* wave. Figure 8 illustrates the network of waves in the three cases. In Cases A1 and A2, the k possible interactions along the initial $\mathscr{P}_s$ wave are sufficient to change it into a *fast* wave, which then escapes. (Note that the final interaction along this $\mathscr{P}_s$ wave, from which the $\mathscr{P}_f$ wave emerges, does not satisfy (2.3); this interaction may be estimated using results from earlier [1].) In Case A1, already $k-1$ or fewer interactions are sufficient to produce the $\mathscr{P}_f$ wave; the second escaping fast wave comes from an $\mathscr{N}_s$ wave that is reflected from the boundary before encountering any positive waves.

Figures 9(*a*) and (*b*) show the asymptotic stress and velocity profiles, respectively, in a case where two $\mathscr{P}_f$ waves escape. In both figures, the quiescent region is $x > 154.4$, the propagation region is $65 < x < 154.4$, the asymptotic region is $4 < x < 65$ and the interaction region is $0 \leqslant x < 4$. In Figure 9(*a*), for $\sigma_0 = -25$, $\sigma_+ = -15$, $\sigma_- = -20$ and $\mu = 0.4$, we have $\sigma_\infty = -18$, as given by formula (3.2*a*). Note that in Figure 9(*b*), however, $v_\infty = -2$, while formula (3.2*b*), if applicable, would predict a value of $(\sigma_0 - \sigma_\infty)/c_s = -7$. The figures therefore illustrate that in the presence of escaping fast waves, formula (3.2*b*) for the asymptotic velocity must be modified.

5 Conclusions

We have studied a periodic stress disturbance, applied at the boundary of a semi-infinite domain, on a fully nonlinear system of differential equations. This system models the

https://doi.org/10.1017/S0956792599004064 Published online by Cambridge University Press

propagation and interaction of shear waves in a saturated granular medium, governed by a hypoplastic flow rule. We found that to the right of a finite-width strip along the boundary, the solution approaches a constant state, $(v_\infty, \sigma_\infty)$, as $t \to \infty$. The structure of the asymptotic solution is thus identical to that of the velocity-controlled problem, studied earlier [1]. In stark contrast to this earlier result, the value of σ_∞ in this paper is independent of both the initial data and the wave speed ratio (see (1.5)), and depends smoothly upon the boundary data. Since the velocity-controlled problem exhibited a wildly discontinuous dependence on its boundary data, it is natural to ask whether this discrepancy between the two problems is capturing a true, physical effect, or is merely a limitation of the model. At present, this question remains unanswered.

Acknowledgements

The authors wish to thank Alistair Fitt for raising important (though still unresolved!) questions regarding the physical origins of differences between the asymptotic stresses for velocity- and stress-controlled boundary conditions.

References

[1] Hayes, B. T. & Schaeffer, D. (1998). Plane shear waves under a periodic boundary disturbance in a saturated granular medium. *Physica D*, **121**, 193–212.

[2] Osinov, V. A. & Gudehus, G. (1996). Plane shear waves and loss of stability in a granular body. *Mechanics of Cohesive–Frictional Materials*, **1**, 25–44.

[3] Gudehus, G. (1997). Attractors, percolation threshholds, and phase limits of granular soils. In: R. Behringer and J. Jenkins (eds.), *Powders and Grains*, Balkema Press.

[4] Osinov, V. A. (1997). Plane waves and dynamic ill-posedness in granular media. In: R. P. Berhinger and J. T. Jenkins, eds., *Powders and Grains 97*, Balkema Press.

[5] Osinov, V. A. (1997). Theoretical investigation of large-amplitude waves in granular soils. *Soil Dynam. Earthquake Engng.*, **17**, 13–28.

https://doi.org/10.1017/S0956792599004064 Published online by Cambridge University Press